

# A chiral lagrangian with Broken Scale: testing the restoration of symmetries in astrophysics and in the laboratory

Luca Bonanno and Alessandro Drago

*Dipartimento di Fisica, Università di Ferrara and  
INFN, Sezione di Ferrara, via Saragat 1, 44100 Ferrara, Italy*

We study matter at high density and temperature using a chiral lagrangian in which the breaking of scale invariance is regulated by the value of a scalar field, called dilaton [1–4]. We provide a phase diagram describing the restoration of chiral and scale symmetries. We show that chiral symmetry is restored at large temperatures, but at low temperatures it remains broken at all densities. We also show that scale invariance is more easily restored at low rather than large baryon densities. The masses of vector mesons scale with the value of the dilaton and their values initially slightly decrease with the density but then they increase again for densities larger than  $\sim 3\rho_0$ . The pion mass increases continuously with the density and at  $\rho_0$  and  $T=0$  its value is  $\sim 30$  MeV larger than in the vacuum. We show that the model is compatible with the bounds stemming from astrophysics, as e.g. the one associated with the maximum mass of a neutron star. The most striking feature of the model is a very significant softening at large densities, which manifests also as a strong reduction of the adiabatic index. While the softening has probably no consequence for Supernova explosion via the direct mechanism, it could modify the signal in gravitational waves associated with the merging of two neutron stars.

PACS numbers: 21.65.Mn, 12.39.Fe, 21.65.Cd, 11.10.Wx

## I. INTRODUCTION

A very hot problem in hadronic and nuclear physics is to investigate the Equation of State (EOS) of matter at large density and/or temperature. Several experiments have been proposed and will likely be performed in the next years. One experiment has been planned at facility FAIR at GSI [5], other experiments could be performed at RHIC (Brookhaven) and at the Nuclatron in Dubna. In all these experiments Heavy Ion Collisions (HICs) will take place at energies of the order of a few ten A GeV, which correspond to the regime at which maximum baryon densities can be reached. Another important source of information concerning matter at high densities is the study of the astrophysics of compact stars, where the temperatures are moderate (typically lower than a few ten MeV), but the baryon density can reach several times nuclear matter saturation density  $\rho_0$ . It is therefore extremely important to investigate the EOS by using various theoretical techniques, providing hints about the main features of matter at those extreme conditions. In a sense one is providing a map of the “new” regions which experiments will likely explore.

In this work we use an effective model for nuclear physics, as a tool for exploring theoretically the unknown regions. The main feature of this model is that it is based on a chiral invariant lagrangian. It is well known that it is not trivial to introduce chiral symmetry in an effective nuclear lagrangian, so that saturation properties of nuclei are well reproduced together with the possibility to restore chiral symmetry at large density and/or temperature. For instance, the attempt of using the linear sigma model to describe nuclear dynamics fails due to the impossibility of reproducing the basic properties of nuclei [6]. The coefficients of the self-couplings of the

scalar field are dictated by the form of the potential and chiral symmetry restoration takes place already at about  $\rho_0$ . More sophisticated approaches have been proposed in the literature. A few works are based on a SU(2) chiral symmetry scheme, either adopting the parity-doublet formulation [7–9] or introducing the scale invariance [10, 11]. Other works extend the symmetry to the strange sector [12–16]. Here we will explore the model introduced by the nuclear physics group of the University of Minnesota [1–4]. In that model chiral fields are present together with a dilaton field which reproduces the breaking of scale symmetry in QCD, but at a mean field level. In their first paper [1] they have shown that it is indeed possible to reproduce the main features of closed shell nuclei; in a second paper [2] the phenomenology of chiral fields, including their interaction with the nuclei, is well described; in a third paper [3] they discuss mesons at finite temperature showing in particular that chiral symmetry is restored at large temperature; finally in Ref. [4] they discuss symmetric nuclear matter at finite density and finite temperature.

In our paper we extend the previous analysis providing rather detailed previsions concerning various quantities which can be measured in the laboratory, like e.g. the compressibility of matter and the behavior of the masses of meson fields at large densities. We will study also the dependence of those quantities on the isospin fraction. Moreover, we will test this chiral model at large baryon and isospin densities which are relevant for studying various astrophysical problems, as the structure and formation of compact stars. In this way we complete the analysis provided in Ref.[17] where we compared the compressibility computed in various nuclear and hadronic models for the EOS of matter.

A few caveats concerning the validity of our results

at very large densities and temperatures are in order: clearly hyperonic and/or quark degrees of freedom should appear in the high energy density regime. On the other hand before investigating even more complicated lagrangians it is worth analyzing in detail the outcome of a purely hadronic model. It is also important to remark that the restoration of scale invariance was analyzed only in Refs. [3, 4] obtaining a unrealistically large critical temperature. In our paper we show that the inclusion of thermal fluctuations of the vector meson fields reduces the critical temperature for scale restoration to a more realistic value and provides a rather new and interesting phase diagram. Hyperons are not included in the present work in order to keep the discussion of chiral symmetry and scale invariance restoration as simple as possible. A more realistic model should incorporate also hyperons, following e.g. the schemes proposed in Refs. [12–16]. Notice finally that the lagrangian we are investigating mimics the behavior of the gluon condensate through the dynamics of the dilaton field. Since the value of the gluon condensate can determine if the system settles in the hadronic or in the quark-gluon phase [18], this model is particularly suitable to be extended to the quark-gluon sector in order to investigate deconfinement, what will be done in a future work.

The structure of the paper is the following. In Sec. II we will describe the model we are using, in Sec. III we discuss the EOS as it can be tested in lab experiments, in Sec. IV we show the implications for astrophysics. Finally, in Sec. V we will present our conclusions.

## II. THE CHIRAL-DILATON MODEL

### A. Scale invariance

The aim of many effective lagrangians for nuclear physics is to mimic the behavior of QCD in the strong regime, where chiral and scale symmetries are broken. While the breaking of chiral symmetry is connected with the generation of fermionic masses, the breaking of scale invariance is due to quantum corrections (the so-called scale or trace anomaly) and is likely associated with the formation of a gluon condensate. More explicitly, the violation of scale invariance in QCD corresponds to a non-conservation of the dilatation current, which reads:

$$\langle \partial_\mu j_{QCD}^\mu \rangle = \theta_\mu^\mu = \frac{\beta(g_s)}{2g_s} F_{\mu\nu}^a(x) F^{a\mu\nu}(x), \quad (1)$$

where  $j_{QCD}^\mu$  is the dilatation current in QCD,  $\theta_\mu^\nu$  is the “improved” energy-momentum tensor,  $F_{\mu\nu}^a(x)$  is the gluon field strength tensor and  $\beta(g_s)$  is the QCD beta function.

In the approach of Schechter, Migdal and Shifman [19, 20] a scalar field representing the gluon condensate is introduced and its dynamics is regulated by a potential chosen so that it reproduces (at mean field level) the

divergence of the scale current which in QCD is given by eq. (1). The potential of the dilaton field is therefore determined by the equation:

$$\theta_\mu^\mu = 4V(\phi) - \phi \frac{\partial V}{\partial \phi} = 4\epsilon_{\text{vac}} \left( \frac{\phi}{\phi_0} \right)^4, \quad (2)$$

where the parameter  $\epsilon_{\text{vac}}$  represents the vacuum energy.

The previous approach holds in the case of pure gauge QCD where, at first loop, the violation of the scale invariance reads:

$$\theta_\mu^\mu = -\frac{11N_c}{96\pi^2} \langle g_s^2 F^2 \rangle, \quad (3)$$

where  $N_c$  is the number of colors. To take into account massless quarks a generalization was proposed in [21], so that also chiral fields contribute to the trace anomaly. In this way the single scalar field of eq. (2) is replaced by a set of scalar fields  $\{\sigma, \pi, \phi\}$ . The relative weight of the gluons and of the quarks to the violation of scale invariance can be read from the QCD  $\beta$ -function, which at first loop is:

$$\beta(g_s) = -\frac{11g_s^3}{16\pi^2} \left( 1 - \frac{2n_f}{33} \right), \quad (4)$$

where  $n_f$  is the number of massless flavors.

### B. The lagrangian

The lagrangian of the chiral-dilaton model (CDM) reads:

$$\begin{aligned} \mathcal{L} = & \frac{1}{2} \partial_\mu \sigma \partial^\mu \sigma + \frac{1}{2} \partial_\mu \pi \cdot \partial^\mu \pi + \frac{1}{2} \partial_\mu \phi \partial^\mu \phi - \frac{1}{4} \omega_{\mu\nu} \omega^{\mu\nu} \\ & - \frac{1}{4} \mathbf{B}_{\mu\nu} \cdot \mathbf{B}_{\mu\nu} + \frac{1}{2} G_{\omega\phi} \phi^2 \omega_\mu \omega^\mu + \frac{1}{2} G_{b\phi} \phi^2 \mathbf{b}_\mu \cdot \mathbf{b}^\mu \\ & + [(G_4)^2 \omega_\mu \omega^\mu]^2 - \mathcal{V} \\ & + \bar{N} \left[ \gamma^\mu (i\partial_\mu - g_\omega \omega_\mu - \frac{1}{2} g_\rho \mathbf{b}_\mu \cdot \boldsymbol{\tau}) - g \sqrt{\sigma^2 + \pi^2} \right] N \end{aligned} \quad (5)$$

where the potential governing the chiral and the dilaton field reads:

$$\begin{aligned} \mathcal{V} = & B\phi^4 \left( \ln \frac{\phi}{\phi_0} - \frac{1}{4} \right) - \frac{1}{2} B\delta\phi^4 \ln \frac{\sigma^2 + \pi^2}{\sigma_0^2} \\ & + \frac{1}{2} B\delta\zeta^2 \phi^2 \left[ \sigma^2 + \pi^2 - \frac{\phi^2}{2\zeta^2} \right] - \frac{3}{4} \epsilon'_1 \\ & - \frac{1}{4} \epsilon'_1 \left( \frac{\phi}{\phi_0} \right)^2 \left[ \frac{4\sigma}{\sigma_0} - 2 \left( \frac{\sigma^2 + \pi^2}{\sigma_0^2} \right) - \left( \frac{\phi}{\phi_0} \right)^2 \right]. \end{aligned} \quad (6)$$

Here  $\sigma$  and  $\pi$  are the chiral fields,  $\phi$  the dilaton field,  $\omega_\mu$  the vector meson field and  $\mathbf{b}_\mu$  the vector-isovector  $\rho$ -meson field, introduced here in order to study asymmetric nuclear matter. The field strength tensors are defined in the usual way  $F_{\mu\nu} = \partial_\mu \omega_\nu - \partial_\nu \omega_\mu$ ,  $\mathbf{B}_{\mu\nu} = \partial_\mu \mathbf{b}_\nu - \partial_\nu \mathbf{b}_\mu$ . The vacuum mean field value of the scalar fields is:

$\bar{\phi} = \phi_0$ ,  $\bar{\sigma} = \sigma_0$  and  $\bar{\pi} = 0$ . Moreover,  $\zeta = \phi_0/\sigma_0$ ,  $B$  and  $\delta$  are constants and  $\epsilon'_1$  is a term which breaks explicitly the chiral invariance of the lagrangian.

It is easy to check that the first two terms of the potential  $\mathcal{V}$  and the chiral symmetry breaking terms contribute to the trace anomaly, so that eq. (2) is satisfied with  $\epsilon_{\text{vac}} = -\frac{1}{4}B\phi_0^4(1-\delta) - \epsilon'_1$ , while the third term fixes the vacuum conditions. Moreover, since  $\epsilon_{\text{vac}}$  takes contributions both from gluons and quarks, the choice  $\delta = \frac{4}{33}$  is suggested by the form of the QCD beta-function at first loop, Eq. (4).

Notice that, as in the case of the well known "Mexican hat" potential, the minimum of the potential  $\mathcal{V}$  is degenerate if  $\epsilon'_1 = 0$  and the ground state satisfies the "chiral circle" equation  $(\sigma^2 + \pi^2)/\sigma_0^2 = \phi^2/\phi_0^2$ . Notice therefore that when the mean value of the dilaton field drops to zero also the radius of the chiral circle drops to zero. In other words, the restoration of scale invariance implies the vanishing of all the condensates, including the chiral one.

It is important to remark that scale invariant masses for the vector mesons can be generated by coupling the vector fields either to the dilaton or to the chiral fields. In the initial versions of the model [21, 22] the coupling  $\frac{1}{2} [G_{\omega\sigma}(\sigma^2 + \pi^2)] \omega_\mu \omega^\mu$  was adopted, which leads to the scenario proposed by Brown and Rho where the vector meson masses scale as the mass of the nucleon [23]. As it will be clarified in the following, that choice leads to an anomalous behavior of the sigma mean field which increases at very large densities. In Ref. [1] a more general combination  $\frac{1}{2} [G_{\omega\phi}\phi^2 + G_{\omega\sigma}(\sigma^2 + \pi^2)] \omega_\mu \omega^\mu$  was tested, but that choice does not provide a good phenomenology for nuclei. In the lagrangian of Eq. (6) the  $\omega$  and  $\rho$  masses are generated by coupling the vector mesons only to the dilaton field so that in the vacuum  $m_\omega = G_{\omega\phi}^{1/2} \phi_0$  and  $m_\rho = G_{\rho\phi}^{1/2} \phi_0$ . This choice, successfully adopted in Refs. [2–4], does not lead to the scenario proposed by Brown and Rho [23].

The values of the parameters which we used for calculations are listed in Table I. They were determined in Ref. [2] by fitting the properties of nuclear matter and finite nuclei. In Ref. [4] two parameter sets are provided, one with  $G_4 = 0$  and the other with  $G_4 \neq 0$ . Since a better phenomenology was obtained with the non-zero value of  $G_4$ , we use that parameter set in our calculations. The value of the coupling constant of the  $\rho$ -meson to the nucleon  $g_\rho$  has been chosen in order to obtain for the symmetry energy at  $\rho_0$  the value  $E_{\text{sym}} = 35$  MeV. The  $\rho$ -meson did not appear in Ref. [4] where only isospin symmetric nuclear matter has been studied.

### C. Thermal fluctuations and their resummation

The main purpose of our work is to study the EOS of nuclear matter at finite temperature. When the temperature is large enough to become comparable to the masses of the meson fields it is mandatory to take into

TABLE I: Values of the parameters.

Quantity	Value
$G_4/g_\omega$	0.19
$ \epsilon_{\text{vac}} ^{1/4}$ (MeV)	228
$g$	9.2
$g_\omega$	12.2
$g_\rho$	8.1
$\zeta = \phi_0/\sigma_0$	1.41
$\sigma_0$ (MeV)	102
$\epsilon'_1{}^{1/4}$ (MeV)	119

account the thermal fluctuations of those fields. In the present work we consider the thermal fluctuations of the chiral fields and of the vector mesons. The fluctuations of the dilaton field are not taken into account in the present paper, due to the large mass of the glueball (about 1.6 GeV). In a future analysis we will consider also the thermal fluctuations of the dilaton field, which become important when studying in detail the temperature-density region where scale invariance is restored.

To take into account thermal fluctuations one has to resort to a technique (developed in Refs.[3, 4]) which allows to deal with non-polynomial functions of the fields. The technique is the following:

a) the chiral invariant combination of the chiral fields is expanded in mean field value plus fluctuations, as:

$$\frac{\sigma^2 + \pi^2}{\sigma_0^2} = \frac{1}{\sigma_0^2}(\bar{\sigma}^2 + 2\bar{\sigma}\Delta\sigma + \Delta\sigma^2 + \pi^2), \quad (7)$$

where  $\bar{\sigma}$  is the sigma mean field value and  $\Delta\sigma$  is its fluctuation. The pion field has a vanishing mean field value and therefore  $\pi^2$  is also the fluctuation squared;

b) in order to simplify the evaluation of the thermal averages of the fluctuations, a crucial assumption is made [3, 4]:

$$\langle \Delta\sigma^2 \rangle \approx \langle \pi_i^2 \rangle. \quad (8)$$

This approximation is based on the observation that at low temperature the fluctuations are small (and therefore the error in assuming the validity of eq. (8) is also small), while at large temperature chiral symmetry is (at least partially) restored and eq. (8) is a sensible approximation. We end up therefore with a unique quantity describing all the thermal fluctuations of the chiral fields,  $\langle \psi^2 \rangle$ , where  $\psi^2 = (\Delta\sigma^2 + \pi^2)/\sigma_0^2$ ;

c) a generic function of the chiral invariant expression is expanded as a series of the field fluctuations and the fluctuations in  $\psi^2$  are taken to all orders [65];

d) to evaluate the numerical value of  $\langle \psi^2 \rangle$  one needs the thermal averages of the fluctuations squared of the chiral fields, which are computed as integrals of the sta-

tistical functions:

$$\langle \pi_a^2 \rangle = \frac{1}{2\pi^2} \int_0^\infty dk \frac{k^2}{e_\pi} \frac{1}{e^{\beta(e_\pi - \mu_a)} - 1} \quad (9)$$

$$\langle \Delta\sigma^2 \rangle = \frac{1}{2\pi^2} \int_0^\infty dk \frac{k^2}{e_\sigma} \frac{1}{e^{\beta e_\sigma} - 1} . \quad (10)$$

e) finally, the series in  $\langle \psi^2 \rangle$  is resummed.

In a more recent paper [24] a new technique to evaluate thermal fluctuations has been developed, in which the fluctuations of  $\sigma$  and  $\pi$  are always considered as independent quantities. In particular, a generic function of  $\sigma$  and  $\pi$  is first expanded as a series of the chiral fields fluctuations and these fluctuations are taken to all orders. The series in  $\langle \Delta\sigma^2 \rangle$  and  $\langle \pi^2 \rangle$  is then resummed. In the case of isospin symmetric matter the fluctuations of the three components of the pionic field are equal and the following result is obtained:

$$\langle f(\bar{\sigma} + \Delta\sigma, \pi^2) \rangle = \int_{-\infty}^{\infty} dz P_\sigma(z) \int_0^\infty dy y^2 P_\pi(y) f(\bar{\sigma} + z, y^2) \quad (11)$$

where

$$P_\sigma(z) = (2\pi \langle \Delta\sigma^2 \rangle)^{-1/2} \exp\left(-\frac{z^2}{2\langle \Delta\sigma^2 \rangle}\right) \\ P_\pi(y) = \sqrt{\frac{2}{\pi}} \left(\frac{3}{\langle \pi^2 \rangle}\right)^{3/2} \exp\left(-\frac{3y^2}{2\langle \pi^2 \rangle}\right) \quad (12)$$

are the gaussian weighting functions. This procedure can be generalized to the case of asymmetric matter, where the fluctuations of the pionic field are independent. In that case instead of the bidimensional integral of Eq. (11) a four dimensional integral is obtained. Notice that the procedure developed in Ref. [24] reduces to the technique discussed in Refs. [3, 4] if the thermal fluctuations of the chiral fields are assumed to be all equal.

In the present work we have mainly adopted the technique of Refs.[3, 4] because our main aim is to

extend the calculations towards asymmetric nuclear matter and astrophysics and we like to be able to directly compare our results with the ones obtained in previous calculations. Most of the results discussed in the following are rather independent from the technique adopted: e.g. the value of the sigma mean field is the same in both cases. Nevertheless it is necessary to use the technique developed in Ref.[24] when computing the isospin splitting of quantities strongly dependent on the thermal fluctuations, in particular the isospin splitting of the mass of the pion.

#### D. Thermodynamics

The value of the fields and of the various thermodynamical quantities at finite temperature and density can be obtained in two ways: i) by solving the field equations (obtained by minimizing the action) and substituting the solutions into the thermodynamical functions or, ii) by minimizing directly the relevant thermodynamical quantities, such as the free energy (if working at given density and temperature), or the thermodynamical potential (if working at given chemical potential and temperature) or the energy density (if working at given entropy and density) [25]. These two approaches are in principle equivalent, although the approximations discussed in the previous subsection can introduce some (small) discrepancy [4]. In the present paper we have decided to minimize directly the thermodynamical quantities because in future works we aim at introducing quark and gluon degrees of freedom. Since in Ref.[18] the pure gluonic sector was described in terms of an effective thermodynamical potential (without introducing a model lagrangian), the second approach is the appropriate one if quarks and gluons are introduced following the scheme proposed in [18].

The thermodynamical potential, within the mean field approximation and taking into account the thermal fluctuations, reads:

$$\begin{aligned} \frac{\Omega}{V} = & \langle \mathcal{V} \rangle - \frac{1}{2} m_\omega^2 \chi^2 \omega_0^2 - \frac{1}{2} m_\rho^2 \chi^2 b_0^2 - G_4^4 \omega_0^4 - \frac{1}{2} m_\sigma^{*2} \langle \Delta\sigma^2 \rangle - \frac{1}{2} m_\pi^{*2} \langle \pi^2 \rangle \\ & + \frac{T}{2\pi^2} \int dk k^2 [\ln(1 - e^{-\beta e_\sigma}) + 3 \ln(1 - e^{-\beta e_\omega})] \\ & + \frac{T}{2\pi^2} \int dk k^2 \left[ \sum_{a=1,3} \ln(1 - e^{-\beta(e_\pi^* - \mu_{\pi a}^*)}) + 3 \sum_{a=1,3} \ln(1 - e^{-\beta(e_\rho^* - \mu_{\rho a}^*)}) \right] \\ & - \frac{T}{\pi^2} \sum_{i=p,n} \int dk_i k_i^2 \left[ \ln(1 + e^{-\beta(E_i^* - \mu_i^*)}) + \ln(1 + e^{-\beta(E_i^* + \mu_i^*)}) \right] , \end{aligned} \quad (13)$$

where the quantities into brackets are thermal averages.

We omit to show explicitly the complicate expression for

$\langle V \rangle$ , which can be obtained using the procedure described in the previous subsection and is given in Eq. (21) of Ref.[3]. The subscripts n and p stay for proton and neutron, respectively, the index  $a$  runs on the three isospin components of the pion and of the  $\rho$ -field and, finally,  $\chi = \phi/\phi_0$ .

The energies which appear into the thermodynamical integrals read  $e_i^* = \sqrt{m_i^{*2} + k^2}$  where  $m_i^*$  is the effective mass of the  $i$ th-field, which can be obtained by computing the thermal average of the second derivative of the lagrangian with respect to the field:

$$M_N^* = g \langle \sqrt{\sigma^2 + \pi^2} \rangle, \quad (14)$$

$$m_\omega^{*2} = m_\omega^2 \chi^2, \quad (15)$$

$$m_\rho^{*2} = m_\rho^2 \chi^2, \quad (16)$$

$$\sigma_0^2 m_\sigma^{*2} = (B_0 \delta + \epsilon'_1) \chi^2 + \left\langle -\frac{B_0 \delta \chi^4 \sigma_0^2}{\sigma^2 + \pi^2} + \frac{2B_0 \delta \chi^4 \sigma_0^2 \sigma^2}{(\sigma^2 + \pi^2)^2} \right\rangle + g \sigma_0^2 (\rho_{Sp} + \rho_{Sn}) \left\langle \frac{1}{\sqrt{\sigma^2 + \pi^2}} - \frac{\sigma^2}{(\sigma^2 + \pi^2)^{3/2}} \right\rangle, \quad (17)$$

$$\sigma_0^2 m_\pi^{*2} = (B_0 \delta + \epsilon'_1) \chi^2 + \left\langle -\frac{B_0 \delta \chi^4 \sigma_0^2}{\sigma^2 + \pi^2} + \frac{2B_0 \delta \chi^4 \sigma_0^2 \pi_a^2}{(\sigma^2 + \pi^2)^2} \right\rangle + g \sigma_0^2 (\rho_{Sp} + \rho_{Sn}) \left\langle \frac{1}{\sqrt{\sigma^2 + \pi^2}} - \frac{\pi_a^2}{(\sigma^2 + \pi^2)^{3/2}} \right\rangle, \quad (18)$$

where  $\rho_{Sp}$  and  $\rho_{Sn}$  are the scalar densities of the protons and of the neutrons, respectively. As already remarked above, we have omitted the thermal average on the dilaton field because its thermal fluctuations are suppressed due to the large mass of this field. Notice that the masses of the chiral fields depend on their thermal fluctuations, which in turn depend on the masses. Due to these complicate dependencies, the minimization of the relevant thermodynamical quantities has to be done iteratively.

Finally, the chemical potentials entering the thermodynamical functions are the effective ones. In the case of the nucleons, the effective chemical potentials are related to the standard ones as follows:

$$\begin{aligned} \mu_p^* &= \mu_p - g_\omega \omega_0 - \frac{1}{2} g_\rho b_0 \\ \mu_n^* &= \mu_n - g_\omega \omega_0 + \frac{1}{2} g_\rho b_0. \end{aligned} \quad (19)$$

Notice that, when asymmetric nuclear matter is considered, the charged isovector mesons acquire a non zero chemical potential, due to the conservation of the isospin charge. The chemical potentials are determined by the equations:

$$\mu_{\pi^+} = \mu_{\rho^+} = \mu_p - \mu_n \quad (20)$$

and the effective ones, which enter e.g. Eq. (13), are given by the relation:

$$\mu_{\pi^+}^* = \mu_{\rho^+}^* = \mu_p^* - \mu_n^* = \mu_p - \mu_n - g_\rho b_0. \quad (21)$$

## E. Goldstone theorem at finite temperature

When discussing a field theory at finite temperature, one has to choose an approximation scheme which do not

violate the symmetries of the lagrangian. In particular, adopting a chiral lagrangian and working in the chiral limit, at  $T=0$  the pion is massless due to the Goldstone theorem. At finite temperature though, it is not automatic that the Goldstone theorem is satisfied, since a wrong truncation can spoil the theorem. There are several contributions to the various observables which one can in principle take into account:

- a) mean field contributions, neglecting all fluctuations;
- b) fluctuations in  $\pi^2$  and  $\sigma^2$ , particularly at finite temperature;
- c) fermionic contributions associated with the so-called particle-hole excitations;
- d) further corrections, as the exchange diagrams discussed e.g. in Ref.[24] at the end of Sec. IVA.

A important guideline in deciding which truncation scheme is appropriate (in other terms, a way for deciding that including a further correction is not necessarily a better approximation) is to check what happens to the Goldstone theorem at finite temperature. For instance, in [3] (which describes the same approximation scheme adopted here) the Goldstone theorem is satisfied also at finite temperature by taking into account contributions a) and b) and neglecting the others (see Fig. 3 of Ref. [3] and Fig. 3 of the present paper). It is well known that, when studying chiral models, another truncation exists which allows the Goldstone theorem to be satisfied at finite temperature and it corresponds to the inclusion of contributions a) and c) (see e.g. [25]). In the chiral limit one can check that indeed the contributions a) and c) to the mass mutually cancel. On the other hand, if one includes a) and b) and c), the Goldstone theorem is *not* satisfied at finite temperature, as already discussed in Ref. [24].

In conclusion, one has to resort either to a) + b) (as we

are doing here) or to a) + c) (as discussed e.g. in [25]). If one wants to add c) to a) and b), other contributions, as the ones in d) has also to be considered in order to satisfy Goldstone theorem.

We will come back to this problem in Sec.IV D, when discussing the possibility that the pions form a Bose-Einstein condensate.

### III. MATTER AT HIGH BARYON DENSITY AND TEMPERATURE

In this section we will focus on nuclear matter calculations at rather high temperature and relatively low isospin asymmetry. These calculations are aimed at providing previsions on the EOS of matter in regions of the energy-density vs. baryon-density plane which can be tested with HIC experiments. Those experiments are particularly interesting at energies of the order of a few ten A GeV, which correspond to the regime at which maximum baryon densities can be reached. In this Section we first discuss the restoration of chiral symmetry and of scale invariance in various region of the energy-density vs. baryon density plane, we then analyze various phenomenological implications of the partial restoration of these two symmetries.

#### A. Phase diagrams

The advantage of using a sophisticated model which includes both the chiral dynamics and the gluon condensate dynamics, is that one can make previsions on the restoration of both the chiral and the scale symmetry. These previsions are different if one considers the case of exact chiral symmetry or the case where a symmetry breaking term is present into the lagrangian. In the following we study both cases.

##### 1. Chiral restoration in the chiral limit ( $\epsilon'_1 = 0$ )

The restoration of chiral symmetry at finite density and temperature. occurs as a first order transition only when the chiral invariance of the lagrangian is exact, or equivalently, only when the explicit symmetry breaking term  $\epsilon'_1 = 0$ . In this case, at a given temperature we observe that for densities larger then a critical one the mean field value of  $\sigma$  drops to zero and the masses of the chiral fields become degenerate. In Fig. 1 the behavior of the  $\sigma$  field, as a function of the density and for various temperatures is displayed. The transition turns out to be first order, due to the discontinuous behavior of the sigma field. Similarly, in Figs. 2, 3 we show the effective masses of the chiral fields, which become degenerate when the symmetry is restored. The chiral phase diagram for isospin symmetric nuclear matter is shown in Fig. 4 in the temperature versus baryon density plane.

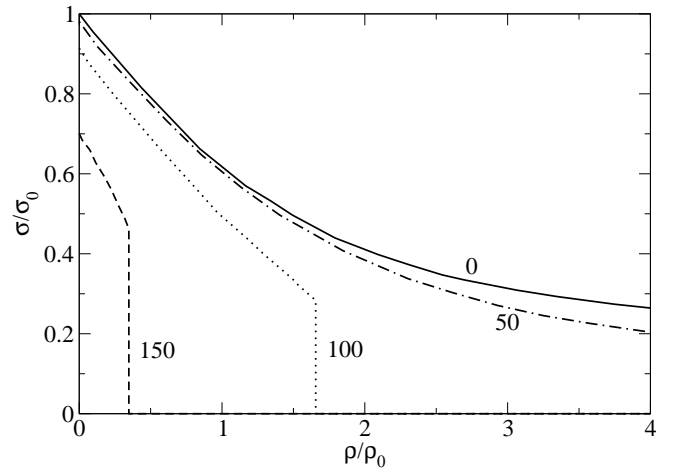


FIG. 1: Mean value of the sigma field as a function of the baryon density for different values of the temperature. Here  $\epsilon'_1 = 0$ .

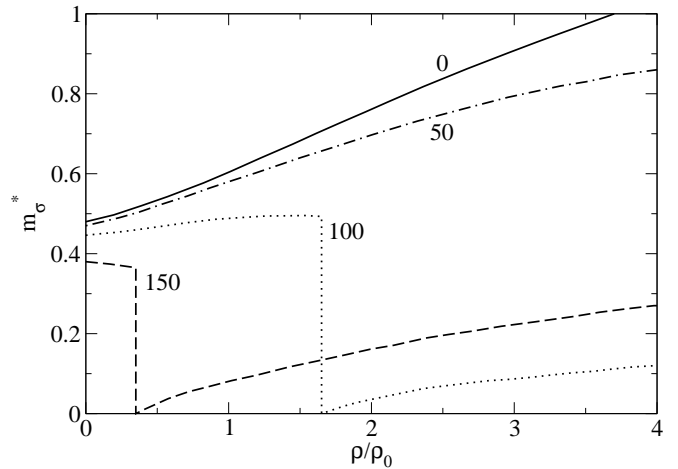


FIG. 2: Effective sigma meson mass as a function of the baryon density for different values of the temperature. Here  $\epsilon'_1 = 0$ .

At zero baryon density the temperature at which the chiral restoration occurs is  $T_C = 165$  MeV, which is rather close to the QCD critical temperature estimated by lattice QCD [26, 27]. Obviously, in the case of QCD the restoration of chiral symmetry comes together with the appearance of the quark-gluon plasma phase. As it can be observed, the critical temperature decreases with increasing density, but it never reaches zero, not even at very large densities. Numerically it tends asymptotically to  $\sim 40$  MeV. It can be interesting to notice that some (very preliminary) lattice calculations at finite density seem to support this result [28]. The chiral phase restoration in the chiral limit is also represented in Fig. 7, in the energy-density vs. baryon-density plane, by two closely spaced solid lines. Since the chiral transition is first order these lines are separated by a small energy gap. Indeed, at finite temperature a first order transition occurs with a jump in the energy density and in the entropy. The temperatures investigated in this Subsection are not

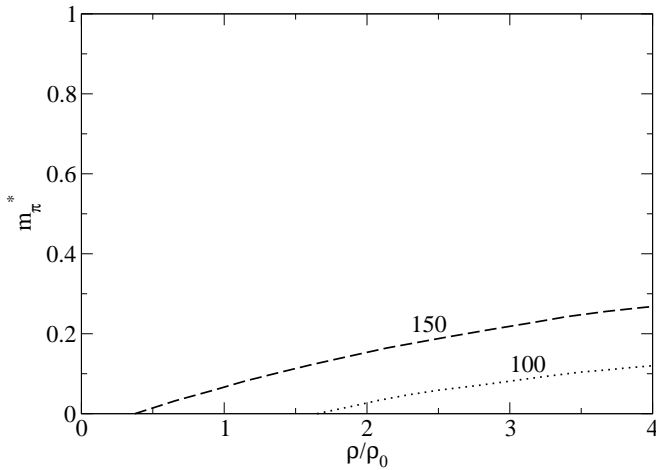


FIG. 3: Effective pion mass as a function of the baryon density for different values of the temperature. Here  $\epsilon'_1 = 0$ .

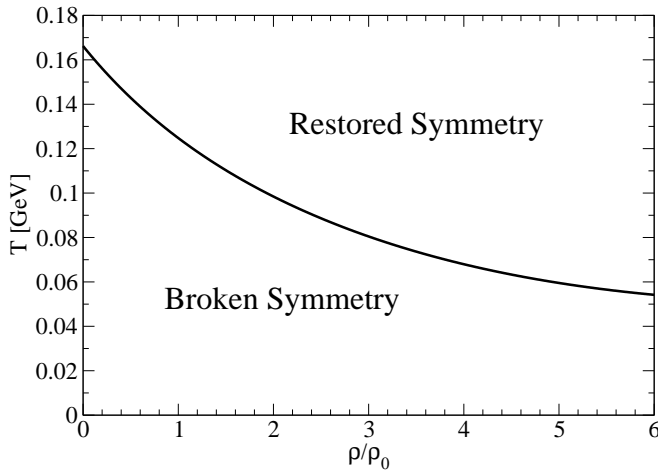


FIG. 4: Chiral phase diagram for symmetric nuclear matter in the temperature versus baryon density plane. Here  $\epsilon'_1 = 0$ .

large enough for the dilaton field to change significantly from its zero temperature value, therefore we could decouple the discussion of chiral symmetry restoration from the restoration of scale invariance. This simplified scenario will not hold in the more realistic  $\epsilon'_1 \neq 0$  case, discussed in the next Subsection.

## 2. Chiral restoration with a chirally broken lagrangian, $\epsilon'_1 \neq 0$

In the more realistic case in which  $\epsilon'_1 \neq 0$  and the pion has a finite mass, we observe that the  $\sigma$  mean field is continuous everywhere and it never drops to zero, at any density as long as  $T \lesssim 196$  MeV, see Fig. 5. Therefore a chiral phase transition, as that observed in the chiral limit case, does not occur. On the other hand, the  $\sigma$  mean field decreases continuously with the density and drops rapidly when the temperature raises from  $T \sim 100$  MeV

to  $T \sim 196$  MeV reaching very small but not vanishing values. This behavior, called “cross over”, is predicted by QCD lattice calculations with two flavors at zero or small densities.

At  $T \gtrsim 196$  MeV the dilaton field drops to zero (initially in the small density region, see Fig. 6) and scale invariance (and therefore also chiral symmetry) is restored, as discussed in the next section.

The large density behavior of the  $\sigma$  mean field can be obtained by solving its equation of motion, what can be done analytically for  $T = 0$ . For large values of the scalar density  $\rho_S$ , we obtain  $\sigma \propto 1/\rho_S$ . Since  $\rho_S$  scales as  $\rho^{1/3}$  for large  $\rho$ , the  $\sigma$  mean field decreases monotonously but slowly with  $\rho$  and it never vanishes. This analytic result remains numerically true also at finite temperatures (for  $T \lesssim 196$  MeV).

Let us now concentrate on Fig. 7, where a sort of “phase map” for symmetric nuclear matter is shown in the energy-density versus baryon-density ( $\rho, \epsilon$ ) plane. The region in which the variation of the  $\sigma$  field is more rapid is indicated by a dashed curve, which is obtained by joining the points of the ( $\rho, \epsilon$ ) plane where the modulus of the derivative of  $\sigma$ , with respect to the temperature, takes its maximum value. In Ref. [29] the maximum energy and baryon densities reached at the moment of maximum compression during a HIC experiment are computed within several models. It is interesting to notice that in all model estimates when the beam energy exceeds  $\sim 5$  A GeV the maximum energy density lies above the dashed line of Fig. 7 and therefore signatures of the partial restoration of chiral symmetry should be observable. In particular, the softening of the EOS due to partial chiral symmetry restoration will be discussed later in this Section.

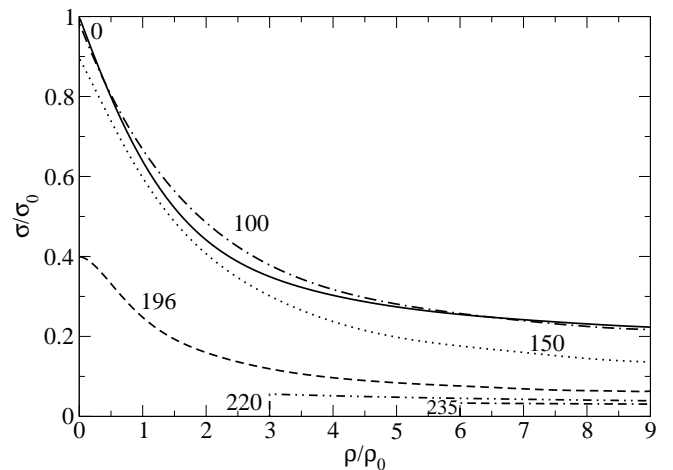


FIG. 5: Same as in Fig.(2), but for the case where the chiral symmetry is explicitly broken ( $\epsilon'_1 \neq 0$ ).

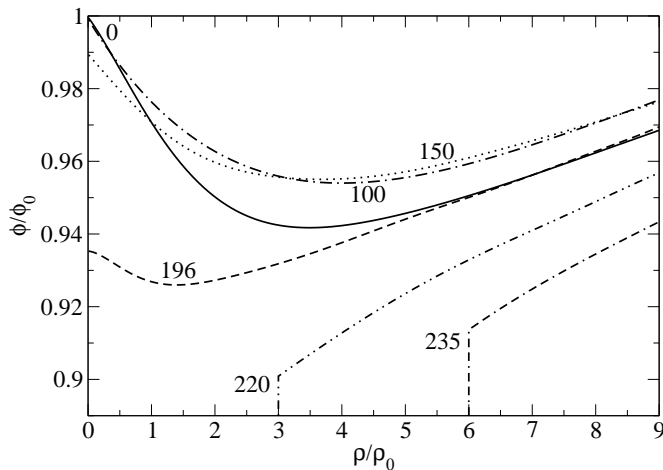


FIG. 6: Mean value of the dilaton field as a function of the baryon density for different values of the temperature. Here  $\epsilon'_1 \neq 0$ .

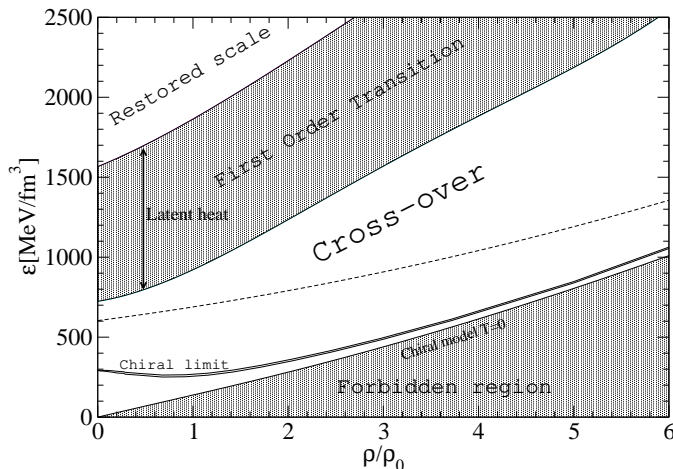


FIG. 7: Phase diagram for symmetric nuclear matter in the energy-density versus baryon-density plane. Two closely spaced solid lines separate the (low-lying) region where chiral symmetry is broken from the (upper-lying) region where chiral symmetry is restored in the chiral limit  $\epsilon'_1 = 0$ . All other graphical signs refer to the broken symmetry case  $\epsilon'_1 \neq 0$ . The lower shaded area indicates the forbidden region under the  $T=0$  EOS. The upper shaded area separates the (low-lying) region where scale symmetry is broken from the region where scale symmetry is restored. The dashed line indicates the maximum (negative) variation of the  $\sigma$ -field mean value with the temperature (see text).

### 3. Scale symmetry restoration

In the model here discussed, the restoration of scale invariance takes place when the mean value of the dilaton field drops to zero. As shown in Fig. 6 the restoration of scale invariance takes place (in the mean field approximation) as a first order transition, signaled by the discontinuous behavior of the dilaton field. A important result, shown in Fig. 7, is that a large energy gap appears between the two phases (due to the large amount of energy released by the condensates which drop to zero). This

gap is of order of 1 GeV/fm<sup>3</sup>, a value not too different from the jump in energy density seen in lattice QCD in the pure gauge sector. Clearly, a direct comparison is meaningless since in full QCD the deconfinement transition (at zero baryon density) is a crossover and, moreover, we do not have quarks in our model.

At zero baryon density, we obtain a critical temperature  $T_c(\rho = 0) \sim 196$  MeV (see Fig. 8), which corresponds to a jump in energy density from  $\epsilon_c^-(\rho = 0) = 725$  MeV/fm<sup>3</sup> to  $\epsilon_c^+(\rho = 0) = 1565$  MeV/fm<sup>3</sup>. This critical temperature is significantly lower than the one estimated in [3, 4]. This reduction is due to the contribution of the vector mesons, which provide a huge contribution to the pressure when the scale invariance is restored (since their masses drop to zero). For instance, in Ref. [3], where no vector meson is present, the scale restoration occurs at  $T \sim 550$  MeV. In Ref. [4] the presence of the  $\omega$  meson lowers the critical temperature to  $T \sim 300$  MeV, while the inclusion in our calculations of the  $\rho$  meson (together with  $\omega$ ) lowers the restoration temperature to  $T \sim 200$  MeV.

We notice from Fig. 7 that the critical energy density  $\epsilon_c(\rho)$  increases with  $\rho$ . Also the critical temperature for scale invariance restoration increases with  $\rho$ , as shown in Fig. 8. This interesting effect arises from the repulsive contribution of the  $\omega$  vector meson, which contributes to the energy density as  $E_\omega = (1/2)(g_\omega/m_\omega^*)^2\rho^2$  (here for simplicity we have assumed  $G_4 = 0$ ). Since the  $\omega$  meson mass scales with the dilaton field (see Eq. (15)),  $E_\omega$  increases when the dilaton field decreases. Therefore at large  $\rho$  it is less convenient to restore scale symmetry [66]. This effect is also clearly visible in Fig. 6 which shows how the dilaton field increases again at large densities.

A few caveats are in order:

- we are working in a mean field approximation and it is well known that the order of a phase transition cannot be determined in that approximation;

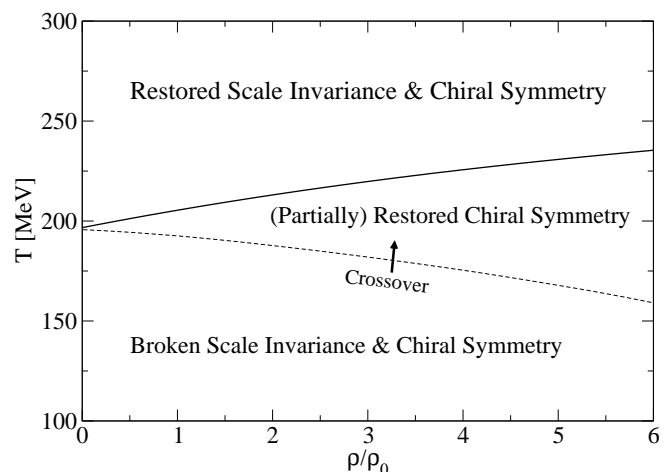


FIG. 8: Phase diagram for symmetric nuclear matter in the temperature versus baryon density plane.



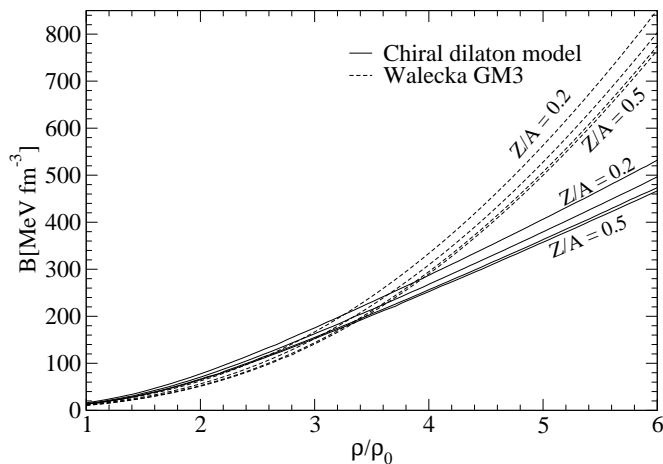


FIG. 9: Bulk modulus  $B = \rho \partial P / \partial \rho$  as a function of the baryon density at  $T=50$  MeV for both the CDM and the Walecka GM3 models. Here various values of the proton ratio are considered.

- at the moment we have not included the thermal fluctuations of the dilaton field, while we have taken into account the thermal fluctuations of the vector mesons. The reason for this choice is that the contribution of the vector mesons largely dominates the contribution of the scalar dilaton field, since the contribution of the vector (isovector) fields is multiplied by their degeneracy. Moreover, to take into account the dilaton thermal contribution one has to overcome the difficulties associated with the logarithmic term. An expansion and resummation similar to the one performed for the chiral fields should be done, what we plan to do in a future work.

## B. Bulk modulus

Here we discuss bulk properties of matter within the CDM. In particular we show in Fig. 9 the value of the bulk modulus  $B = \rho \partial P / \partial \rho$  as a function of  $\rho$  at  $T=50$  MeV. Here the calculations are performed for various isospin densities and we compare with the same quantity computed within the Walecka GM3 model [30]. Notice that the bulk modulus computed with the CDM is larger than the one calculated with GM3 when  $\rho \lesssim 3\rho_0$ . This is due to the larger value of the CDM incompressibility parameter at  $\rho_0$  ( $K^{-1} = 9\rho^2 \frac{\partial^2 E/A}{\partial \rho^2} = 322$  MeV) compared with that obtained using GM3 ( $k^{-1} = 240$  MeV).

Observe that for  $\rho \gtrsim 3\rho_0$  the effect of the partial restoration of the chiral symmetry manifests as a softening of the EOS. This softening is clearly visible in Fig. 9 where the bulk modulus computed with the CDM equals the one evaluated using GM3 at about  $3\rho_0$  and becomes smaller for larger values of  $\rho$ . The effect of the isospin density is to increase the bulk modulus, since the  $\rho$  meson gives a positive contribution to the pressure proportional

to the baryon density. The increase of the bulk modulus when moving from  $Z/A=0.5$  to  $Z/A=0.2$  is of about 10% both for the CDM and for GM3.

The dependence of the bulk modulus on the density and the temperature can be measured in HIC experiments, in particular by analyzing the so called collective flows. A first attempt has been done in Ref. [31], where they have extracted the value of the incompressibility parameter from HIC experiments, observing a significant softening of the EOS when the beam energy varies from 2 A GeV up to 10 A GeV. By comparing with the CDM one can notice that this softening can be interpreted as due to partial chiral symmetry restoration if densities of at least  $6 - 7\rho_0$  are reached during a HIC. In Ref.[17] we have shown that if such large densities are not reached, then this softening can better be interpreted as due to the formation of a mixed hadron-quark phase.

## C. Effective meson masses

A very important point concerns the predictions of the CDM about the experimentally measurable “in medium” masses, as the vector meson masses and the pion mass, whose expressions are provided in Eqs. (15,16,18).

### 1. Effective pion mass

The binding energy of the deeply bound 1s and 2p states in pionic atoms of  $^{207}\text{Pb}$ , established experimentally through the  $^{207}\text{Pb}(d,^3\text{He})$  reaction, has been used to derive the value of the pion mass at nuclear matter density [32, 33]. The result of this still preliminary analysis is that the pion mass increases by about 28 MeV at  $\rho_0$  in symmetric nuclear matter.

In Fig. 10a the pion effective mass in symmetric nuclear matter is plotted as a function of the baryon density and for different values of the temperature. We observe that the pion mass increases monotonously with the baryon density reaching a value of about 167 MeV at  $\rho_0$  and  $T = 0$ , a result very close to the one suggested in Refs.[32, 33]. We also compare the technique of Refs. [3, 4] with the technique of Ref. [24] (see the previous discussion in subsection IIC). Most of the results obtained in the present work are almost independent of which technique is adopted, but the masses of the chiral fields are very delicate and the two techniques provide different results even in the case of isospin symmetric matter, as we show in Fig. 10a

In Fig. 10b we show the effect of the isospin asymmetry ( $Z/A=0.3$ ) on the pion mass. Notice that in isospin asymmetric matter the positive and negative pions have opposite (nonzero) chemical potentials. Then, according to Eq. (9), their thermal fluctuations are different as well as their effective masses, defined by Eq. (18). In order to consider this effect, in our calculations we used the technique of Ref. [24]. In Fig. 10b we show that the

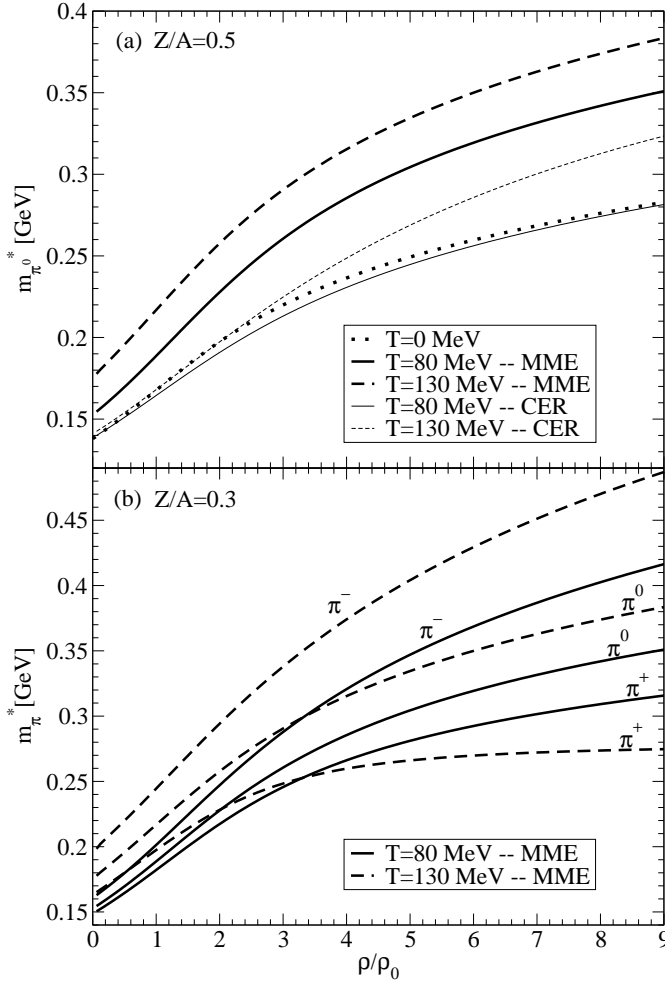


FIG. 10: In panel (a) the pion effective mass obtained using the technique of Ref. [24] (MME, thick lines) is compared with the mass obtained using Refs. [3, 4] (CER, thin lines). The mass is plotted as a function of the baryon density, for  $Z/A=0.5$  and for three values of the temperature. The two techniques are equivalent at  $T=0$ . In panel (b) we show the masses of the different isospin components of the pion, as a function of the baryon density, for  $Z/A=0.3$  and for two values of the temperature. Here we adopted the technique of Ref. [24]. At  $T=0$  no isospin mass splitting is present.

mass splitting of the different pion components increases substantially with the density and with the temperature (the mass splitting vanishes at  $T=0$ ). In particular, at  $\rho = 3\rho_0$  and  $T=130$  MeV, the difference between  $m_{\pi^-}$  and  $m_{\pi^+}$  reaches a value of about 100 MeV. Notice that this result, obtained without including any contribution associated with the so-called particle-hole excitations, is comparable to the isospin splitting of the pion mass associated with the so-called Tomozawa-Weinberg term.

## 2. In medium vector meson masses

The experimental determination of the in-medium modification of the light vector mesons ( $\omega$ ,  $\rho$  and  $\Phi$ )

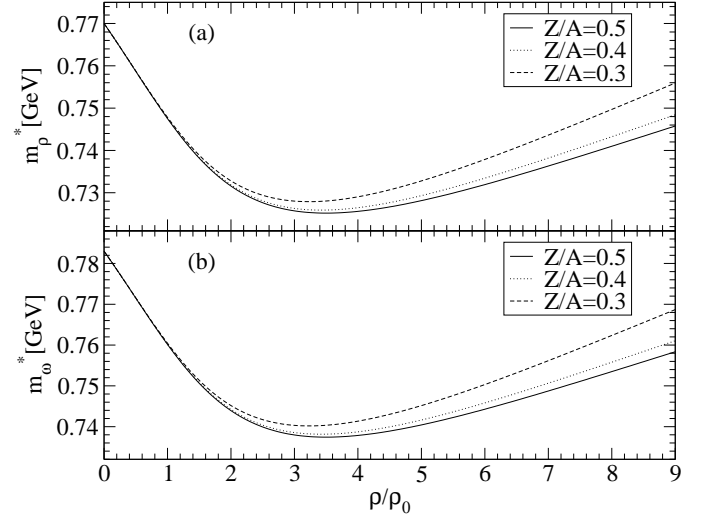


FIG. 11: Vector meson masses as a function of the baryon density at  $T=0$  and for different proton fractions.

is still uncertain. Recent experiments have advanced to a level that in-medium spectral information on vector mesons can be deduced. Experimentally, the best approach is the dilepton spectroscopy, in particular the investigation of the dileptonic decay modes of the light vector mesons, produced off nuclei or in HICs. In Fig. 11 the masses of the vector mesons  $\omega$  and  $\rho$ , evaluated within the CDM, are plotted as functions of the baryon density at zero temperature, and for different values of the proton ratio. We do not show the values of the vector mesons masses for temperatures different from zero because, up to  $T \sim 150$  MeV, the masses vary only slightly with the temperature (the differences are of a few per cent).

Notice the peculiar behavior of  $m_{\omega}$  and  $m_{\rho}$  with  $\rho$ : for low densities the masses initially drop, reaching a minimum in the neighbor of  $\rho = 3.5\rho_0$ , while for higher values of  $\rho$ , the masses increase again. This effect is due to the difficulty in restoring the scale invariance at large densities, as discussed in subsection III A 3. The special scenario obtained within the CDM seems to be in agreement with several experimental analysis indicating a moderate reduction of the masses of the vector mesons at densities of the order of  $\rho_0$  and no significant reduction when the masses are tested at very large densities.

For instance, in experiments of scattering of photons and protons on nuclei, densities about  $\rho_0$  are tested and the results indicate a drop of the  $\omega$ -mass by 14% at saturation density (CBELSA/TAPS) [34]. More controversial is the situation concerning the  $\rho$ -mass: the KEK-PS E325 collaboration indicates a drop by 9% at  $\rho_0$  [35, 36] while a recent experiment at JLAB suggests a smaller drop by  $\sim 2\%$  at  $\rho_0$  [37]. On the other hand, in HIC experiments at energies of the order of one hundred A GeV (SPS and NA60), the vector mesons mass shift has been found to vanish [36, 38, 39]. This result presumably discards the scenario predicted by Brown and Rho [36, 40], where the vector meson masses drop continuously with the density

[23].

Finally, the effect of a finite isospin density is to increase the vector masses as it can be observed in Fig. 11. This effect grows with the baryon density, although at  $\rho = 9\rho_0$  the increment is only of about 1% for both the vector meson masses.

#### IV. ASTROPHYSICAL APPLICATIONS

Neutron Stars (NSs) are the most dense objects in nature while their temperature is always below a few ten MeV and typically lower than one MeV. Therefore they are the only objects which can provide information on the EOS of matter at very large densities and low temperature. Unfortunately the structure of compact stars is still uncertain since astrophysical data can provide only rather indirect indications, leaving the field open to theoretical investigations based on models for the high density EOS. Since the CDM is a chiral model, it is very interesting to investigate its provisions concerning matter at very large densities and small temperatures. In particular it is possible to explore how the chiral dynamics can affect the structure and the formation of a NS. The dynamics of the gluon condensate does not play a crucial role at low temperatures. In this section we compute the value of the adiabatic index which plays a crucial role in Supernova explosions and we investigate within the CDM the structure of NSs [16].

In order to better understand the formation and the structure of a NS we also discuss the effective masses of the various fields and, finally, we consider the possibility to reach the pion condensation in NSs.

##### A. Adiabatic index

As far as we know, the explosion of a core-collapse supernova proceeds as the following (for a recent review see Ref. [41]): when a massive star exhausts its nuclear fuel, the gravitational force cannot be contrasted by the outward pressure and the core starts to collapse. During this stage, which typically last much less than a second, the pressure strongly exceeds the electron degeneration pressure and neutronization occurs. The temperature is of the order of few ten MeV and the neutrinos cannot escape from the collapsing matter since their cross section is very large. The lepton number is then conserved and no energy can escape the system, giving the possibility to describe the entire process as an adiabatic compression with a entropy per baryon of the order of unity. Moreover, since the time scale of the  $\beta$  interactions is of the order of  $10^{-8}$  s, the system has the time to reach the  $\beta$ -equilibrium. When the density of the core overcomes  $\rho_0$ , due to the nuclear repulsion the core bounces triggering a shock wave which propagates to the outer layers of the star. In hydrodynamical simulations, it turns out that the shock wave stalls while it is still propagating

inside the outer layers of the progenitor star. Therefore the so called “direct mechanism”, characterized by the idea that the explosion is directly related to the shock wave generated by the bounce, has been ruled out. The failure of this direct mechanism sets the stage for a ‘delayed’ mechanism, in which the shock is re-energized by the heating of the outer layers due to the intense neutrino flux emerging from the neutrino-sphere.

It is worth discussing more in details the conditions under which the direct mechanism would be successful. It has been noticed that the possibility for a supernova to explode via the “direct mechanism” is related to the softening of the EOS at densities just above  $\rho_0$  [42]. This possibility, exploited in the Baron-Cooperstein-Kahana (BCK) EOS [43] has been discarded because it seems to be inconsistent with the constraints on the NS masses coming from observations, since a too soft EOS cannot support a sufficiently massive NS. A more sophisticated approach invokes a softening taking place only in a finite density window and associated with a phase transition. In this way the EOS can be stiff again at densities larger than the ones associated with the transition. This possibility is also not new and it has been investigated in several papers [44–47]. In all those works a strong softening of the EOS is ascribed to a phase transition which can be due either to the pion condensation or to the formation of a mixed phase of hadrons and quarks. Since in the CDM we obtain a softening of the EOS at moderate densities due to chiral symmetry restoration it is worth to explore the possible influence of this transition on the supernova explosion.

In order to investigate the core collapse of a massive star, we compute the EOS along adiabatic paths for matter composed of neutrons, protons, electrons and electronic neutrinos. Due to the previous considerations, the conditions imposed to the system are:

i) leptonic number conservation:

$$\rho_e + \rho_{\nu_e} = Y_{le}(\rho_p + \rho_n) \quad (22)$$

ii) electric charge neutrality:

$$\rho_p = \rho_e \quad (23)$$

iii)  $\beta$ -equilibrium:

$$\mu_n - \mu_p = \mu_e - \mu_{\nu_e} \quad (24)$$

where  $Y_{le} = 0.4$  is the constant ratio of the leptonic density to the baryon density. Since before the collapse no muons are present, we keep  $Y_{l\mu} = \frac{\rho_\mu + \rho_{\nu_\mu}}{\rho} = 0$ .

An important quantity which allows to estimate the softness of the EOS is the adiabatic index, which is defined as:

$$\Gamma = \frac{\partial \ln P}{\partial \ln \rho} \quad (25)$$

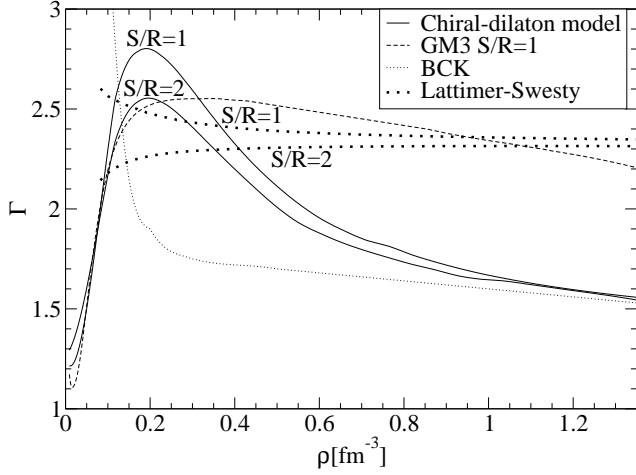


FIG. 12: Adiabatic index as a function of  $\rho$  computed within various models for isentropic  $n, p, e^-, \nu_e$  matter with  $Y_{le} = 0.4$ .

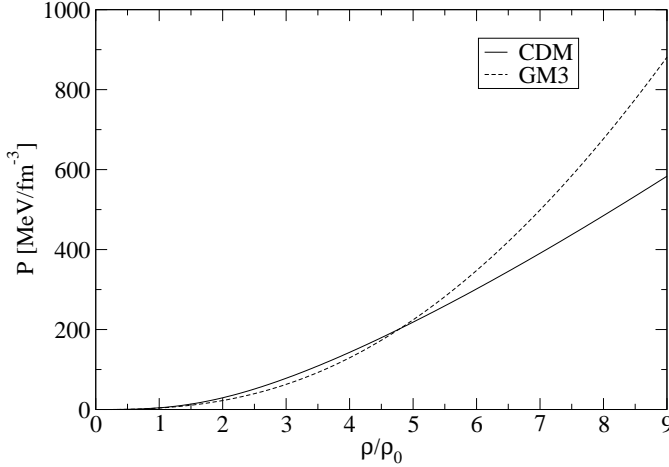


FIG. 13: Pressure for NS matter as a function of baryon density, evaluated within the CDM and within the Walecka GM3 model.

where  $P$  is the pressure. It corresponds to the index of a polytropic equation of state  $P(\rho) = P_0 \left( \frac{\rho}{\rho_0} \right)^\Gamma$ . In Fig. 12 we show  $\Gamma$ , obtained from the CDM EOS and from other models, as a function of  $\rho$ . Notice that within the Walecka GM3 and the Lattimer-Swesty EOS [48] no significant reduction of  $\Gamma$  is observed at supranuclear densities. At the contrary, the strong softening occurring within the BCK EOS [43] at densities just above  $\rho_0$  allows a supernova to explode via the “direct mechanism” (recall that the BCK EOS has been ruled out since it provides too low NS masses). Within the CDM the partial restoration of chiral symmetry manifests as a strong softening of the EOS (see Fig. 13). This softening is also observed as a strong reduction of  $\Gamma$  for densities larger than  $3\rho_0$ . Although this reduction is comparable with that obtained in BCK, since the density at which it occurs is much larger than  $\rho_0$  we do not expect that the CDM can allow a supernova to explode via the “direct

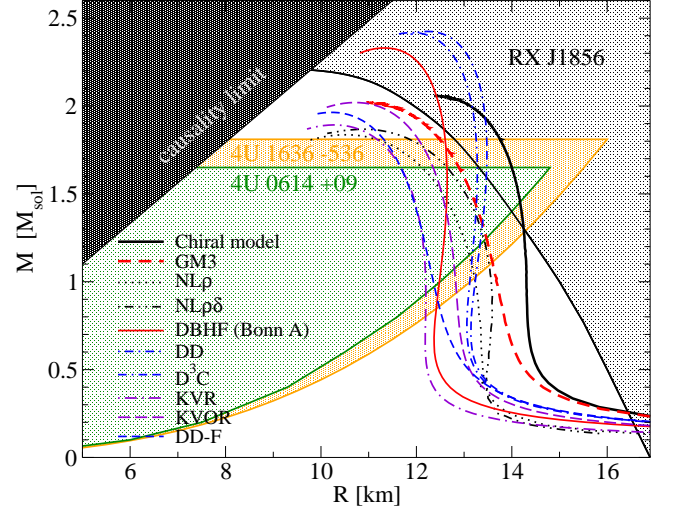


FIG. 14: (Color online) Mass-radius relation for the CDM and for various other models together with recent experimental constraints. Adapted from Ref. [49].

mechanism”. On the other hand, since very large densities are reached during the collapse of a binary system of neutron stars, we expect that such a strong decrease of  $\Gamma$  can have interesting consequences, for instance in affecting the gravitational wave signal emitted just before the formation of the black-hole [50].

## B. Neutron stars

A NS is the cold remnant of the explosion of a core-collapse supernova and it is composed by neutrons, protons, electrons and muons in  $\beta$ -equilibrium. Since the temperature is very low the neutrinos cross section is very small, allowing the neutrinos produced by  $\beta$ -decay to escape from the star. Therefore the lepton number is not conserved. Since electric charge neutrality has also to be imposed, the conditions defining NS matter read:

$$\begin{aligned}\mu_n &= \mu_p + \mu_e \\ \mu_n &= \mu_p + \mu_\mu \\ \rho_p &= \rho_e + \rho_\mu.\end{aligned}\tag{26}$$

That EOS is then used to solve the Tolman-Oppenheimer-Volkov (TOV) equation obtaining a sequence of stable stellar configuration.

The mass-radius relations for the CDM and various other models are shown in Fig. 14, together with several recent experimental constraints coming from observations and discussed in Ref. [49]. The models considered in Fig. 14 can be separated into Relativistic Mean Field (RMF) phenomenological models, including the Walecka type models (GM3 [30], NLp [51] and NLpδ [52]) and those with density dependent coupling constants (DD [53],  $D^3C$  and DD-F [49, 54]), the “ab-initio” calcula-

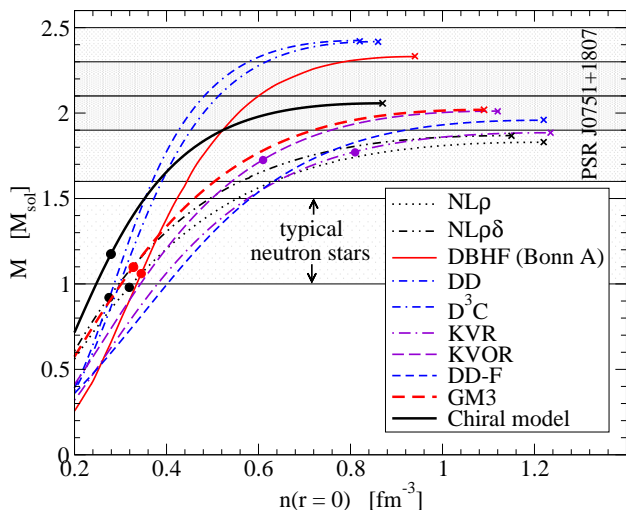


FIG. 15: (Color online) NS mass vs. central density for the same models of Fig. 14. The full circles indicate the DU thresholds and the stars indicate the maximum mass configurations. Adapted from Ref. [49].

tions including the relativistic Dirac-Brueckner-Hartree-Fock (DBHF [55–58]) and the hybrid models (KVR and KVOR [59, 60]) which bridge the gap between the fully microscopic and more phenomenological descriptions.

The experimental constraints are extracted from observations of kilohertz quasi-periodic brightness oscillations in the Low Mass X-Binaries 4U 0614+09 and 4U 1636-536 and from the thermal radiation of the isolated NS source RX J1856.5-3754.

Due to the rather unrealistically large value of the incompressibility parameter at  $\rho_0$  ( $K^{-1}=322$  MeV), larger NS radii are obtained within the CDM than within the other models. Therefore, although the CDM allows to have a NS with a mass  $M \sim 1.4M_\odot$  and a radius of 14 Km, satisfying the constraints from RX J1856 (the other models exclude this interpretation), our result is questionable due to the too large value of the incompressibility at saturation.

An important check is based on the recent observations of PSR J0751+1807. The data analysis, although still uncertain, allows to extract a NS mass of  $2.1 \pm 0.2$  ( $^{+0.4}_{-0.5}$ )  $M_\odot$  (first error estimate with  $1\sigma$  confidence, second in brackets with  $2\sigma$  confidence) [61]. Since the CDM exhibits a maximum mass  $M = 2.06M_\odot$  this constraint is easily fulfilled. The constraint is displayed in Fig. 15 where the NS mass vs. central density relation is shown for the same models of Fig. 14 and where the crosses denote the maximum mass configurations.

When discussing NSs a very important role is played by the cooling mechanism. We can roughly divide the cooling mechanisms in “slow” ones, as e.g. the so-called modified Urca process, and fast ones, as e.g. the Direct Urca (DU) process which corresponds to a sequence of neutron  $\beta$ -decays and lepton captures (see e.g. Ref. ([62])). From simple considerations it is possible to find the crit-

ical baryon density beyond which the DU processes can occur in a NS, which turns out to be the density at which the proton ratio in NS matter reaches the value:

$$x_{DU} = \frac{1}{1 + (1 + x_e^{1/3})^3} \quad (27)$$

where  $x_e = \frac{\rho_e}{\rho_e + \rho_\mu}$ . In Fig. 15 the DU-thresholds are denoted by full circles. Notice that, although the CDM allows the DU to occur for NS masses exceeding  $\sim 1.2M_\odot$ , its threshold is slightly higher than those obtained within GM3, NL $\rho$ , NL $\rho\delta$  and DBHF.

Finally, the effect of the softening of the CDM EOS manifests as an “anomalous” behavior of the NS sequence with respect to the other models. Notice in fact that in Fig. 15 at low central densities the CDM NS masses are rather large and the CDM sequence seems to follow the trend of the *DD*, *D<sup>3</sup>C* and *DBHF* models whose maximum mass configurations exceed  $2.3M_\odot$ . However at larger central densities the sequence flattens and a maximum mass only slightly larger than GM3 is reached ( $M_{max} = 2.06M_\odot$ ).

### C. In medium masses

In order to understand how the partial restoration of chiral symmetry affects the structure of NSs, we computed, within the CDM and using the technique developed in Ref. [24], the  $\pi^0$  and  $\sigma$  meson effective masses as a function of  $\rho$  both for NS matter and for isoentropic neutrino-trapped matter (see Fig. 16). We find that even at large densities the masses of the two chiral fields are still rather different, although the mass of  $\pi^0$  is considerably larger than in the vacuum. The effect of the temperature on the partial restoration of chiral symmetry is very small but it can anyway be noticed by comparing the isoentropic curves with  $S/R=1$  and  $S/R=2$ : for the larger value of the entropy the  $\sigma$  and  $\pi^0$  masses start getting closer, the  $\sigma$  mass by decreasing and the  $\pi^0$  mass by increasing its value.

Finally, we have examined the in-medium modification of the nucleon and of the pion mass by plotting their values as a function of the radius in the case of a spherical non-rotating NS of mass  $M = 1.4M_\odot$ , see Fig. 17 (notice that, although in presence of isospin asymmetry, at  $T=0$  it comes out that  $m_{\pi^0} = m_{\pi^+} = m_{\pi^-} \equiv m_\pi$ ). The value of nucleon mass decreases by more than 50% when going from the outer crust to the center of the star. The pion mass, at the contrary, increases by about 45%.

### D. Pion condensate

Since in compact stars very large baryon densities and isospin asymmetries are reached, it is interesting to investigate the possibility to form a meson Bose-Einstein Condensate (BEC). In particular we investigate here the

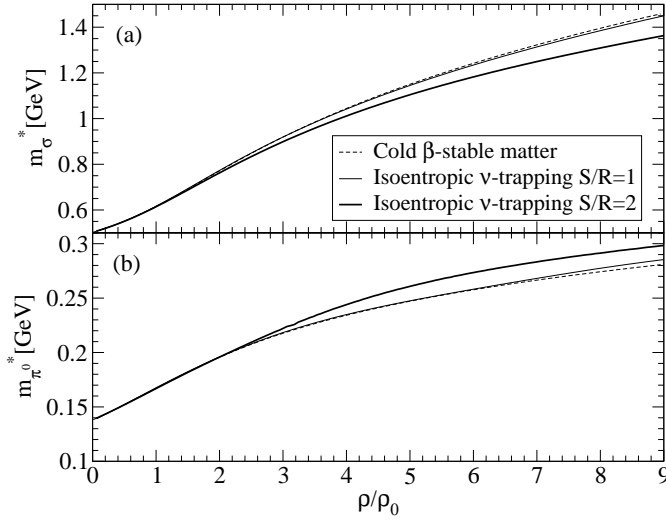


FIG. 16:  $\sigma$  (figure (a)) and  $\pi^0$  (figure (b)) effective masses as a function of the baryon density for NS matter (dashed line) and for isoentropic  $\nu$ -trapped matter with entropy per nucleon  $S/R=1$  (thin solid line) and  $S/R=2$  (bold solid line).

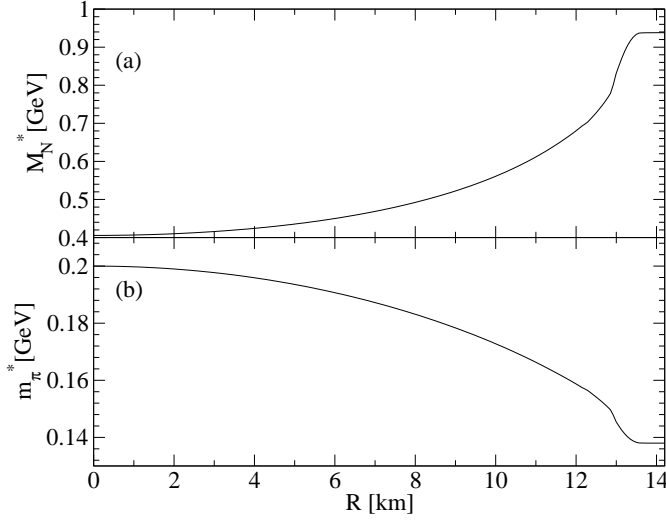


FIG. 17: In-medium mass modification of the nucleon (figure (a)) and of the pion (figure (b)) inside a neutron star of  $1.4 M_\odot$ .

possibility of reaching the pion BEC, which is easier to achieve due to the small value of the pion mass. Usually with “pion condensate” one refers to a collective pionic excitation at non zero-momentum. This collective state is a pole in the pion propagator modified by the inclusion of the particle-hole excitations. In this work we do not include the particle-hole excitations in order to satisfy the Goldstone theorem at finite temperature (see the discussion in section II E) and we call “pion condensate” the zero-momentum Bose-Einstein condensate of pions.

Recall that in order to conserve the isospin charge a chemical potential is assigned to the pions, which reads:

$$\mu_{\pi^+} = \mu_p - \mu_n, \quad (28)$$

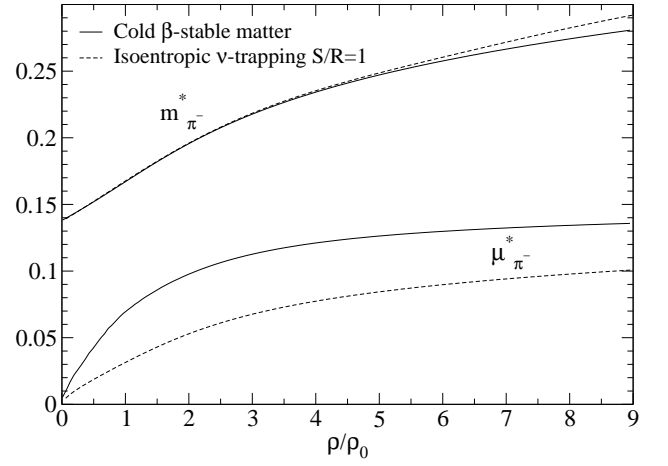


FIG. 18:  $\pi^-$  effective mass and effective chemical potential as a function of the baryon density, computed within the CDM for NS matter and for isoentropic  $\nu$ -trapped matter with entropy per baryon  $S/R=1$ .

where  $\mu_p$  and  $\mu_n$  are the chemical potential of protons and neutrons, respectively. The equation above assures the equilibrium in the reaction  $n \leftrightarrow p + \pi^-$ . Moreover the pion effective chemical potential, which enters the thermodynamical integrals, is given by:

$$\mu_{\pi^+}^* = \mu_p^* - \mu_n^*, \quad (29)$$

where  $\mu_p^*$  and  $\mu_n^*$  are the effective chemical potential of protons and neutrons respectively, given by Eq. (19). The effective chemical potential of the pion increases with the baryon density and with the isospin asymmetry. When the effective chemical potential becomes equal to the pion effective mass, real pions start to be produced in the medium and they condense in the state of minimum energy, i.e. the zero momentum mode. The condition for the onset of the pion BEC then reads [25]:

$$\mu_{\pi^-}^* = m_{\pi^-}^*. \quad (30)$$

In Fig. 18 the  $\pi^-$  effective mass and its effective chemical potential (computed using the technique developed in Ref. [24]) are plotted as a function of  $\rho$ . Here we consider two different cases:  $\beta$ -stable NS matter at  $T=0$  and isoentropic  $\nu$ -trapped matter at  $\beta$ -equilibrium with entropy per baryon  $S/R=1$ . As it can be seen the  $\pi^-$  mass grows with  $\rho$  and it does not change appreciably between the two cases. Also  $\mu_{\pi^-}$  increases with  $\rho$ , but its value actually depends on the value of the entropy and on neutrino-trapping.

The important result is that the condition for the onset of the BEC is never achieved, not even at large densities. This is due to the increase of the pion effective mass with  $\rho$ , which remains always larger than the chemical potential. In simpler models, like e.g. the Walecka GM3 where the pion mass is constant, the increase of the chemical potential gives rise to the pion condensation, as discussed in Ref. [63].

## V. CONCLUSIONS

The main aim of this work was to investigate the behavior of matter at large densities and temperatures by using an effective lagrangian with broken scale invariance and chiral symmetry. Our results are concordant with those obtained in Refs. [3, 4]. We extended the previous calculations in several directions and wherever possible we compared with experimental data. We have also used two different techniques to evaluate the effects of thermal fluctuations, i.e. the method developed in Refs. [3, 4] versus the one developed in Ref. [24]. The latter is more general since it does not make any assumption concerning the value of the thermal fluctuations of the chiral fields. The two techniques provide similar results as long as we are not investigating subtle isospin dependencies such as the mass splitting of the isospin components of the pion.

Our main results are the following:

- we have provided a phase diagram mapping the regions in which chiral symmetry and/or scale invariance are restored. The scenario provided by the model we have studied, i.e. the decoupling of chiral symmetry restoration and scale invariance restoration (which is likely associated with deconfinement) shares strong similarities with the scenario recently suggested by McLerran and Pisarski in the large  $N_c$  limit [64];
- the masses of vector mesons are affected by the partial restoration of scale invariance, since they scale with the dilaton field. Therefore scale invariance restoration is more difficult at large densities, because the repulsive effect of the exchange of vector mesons is enhanced if their mass is reduced;
- the masses of the vector mesons first reduce at finite density, but at larger densities they even increase. This result holds up to temperatures of the order of 200 MeV, at even larger temperatures scale invariance starts being restored and the vector meson masses drop to zero;
- In isospin symmetric matter the pion mass increases

with the density and with the temperature. At  $\rho_0$  and  $T=0$  the effective mass of the pion is about 170 MeV.

In presence of isospin asymmetry the masses of the different pion components split. The splitting increases with the density and the temperature and, for instance, at  $\rho = 3\rho_0$ ,  $T=130$  MeV and  $Z/A=0.3$   $m_{\pi^-} - m_{\pi^+} \sim 100$  MeV;

– a very substantial reduction of the adiabatic index takes place at densities exceeding  $3\rho_0$ . Although this softening cannot directly affect the mechanism of Supernova explosion, because it starts at too large densities, its signature could be observed during a two neutron star merging;

– the BEC of pions does not form in NSs due to the increase of the pion mass with the density.

The present work can be extended in several directions. In particular the restoration of scale invariance will be better investigated by including in the calculation also the thermal contribution of the dilaton field, while in the present work we have only taken into account the mean field effect. Hyperons should also be included in the model. This direction is now explored by analysis similar to ours and performed by the Frankfurt group [16]. The most interesting extension would be to take into account quark degrees of freedom. An attempt in that direction is a recent paper in which deconfinement is discussed in a dilaton model, but in the pure gauge sector [18].

## VI. ACKNOWLEDGMENTS

It is a pleasure to thank Veronica Dexheimer, Jürgen Schaffner-Bielich and Raffaele Tripiccionone for many useful discussions, David Blaschke and Thomas Klähn for providing data used in many figures. We are particularly grateful to Andrea Lavagno, with whom most of the problems investigated in the work have been extensively analyzed.

- 
- [1] E. K. Heide, S. Rudaz, and P. J. Ellis, Nucl. Phys. **A571**, 713 (1994).
  - [2] G. W. Carter, P. J. Ellis, and S. Rudaz, Nucl. Phys. **A603**, 367 (1996).
  - [3] G. W. Carter, P. J. Ellis, and S. Rudaz, Nucl. Phys. **A618**, 317 (1997).
  - [4] G. W. Carter and P. J. Ellis, Nucl. Phys. **A628**, 325 (1998).
  - [5] P. Senger, J. Phys. **G30**, S1087 (2004).
  - [6] R. J. Furnstahl, B. D. Serot, and H.-B. Tang, Nucl. Phys. **A598**, 539 (1996).
  - [7] V. Dexheimer, S. Schramm, and D. Zschesche, Phys. Rev. **C77**, 025803 (2008).
  - [8] V. Dexheimer, S. Schramm, and H. Stoecker (2008), arXiv:0801.2523 [astro-ph].
  - [9] V. Dexheimer, G. Pagliara, L. Tolos, J. Schaffner-Bielich, and S. Schramm, Eur. Phys. J. **A38**, 105 (2008).
  - [10] I. Mishustin, J. Bondorf, and M. Rho, Nucl. Phys. **A555**, 215 (1993).
  - [11] R. J. Furnstahl, H.-B. Tang, and B. D. Serot, Phys. Rev. **C52**, 1368 (1995).
  - [12] P. Papazoglou, S. Schramm, J. Schaffner-Bielich, H. Stoecker, and W. Greiner, Phys. Rev. **C57**, 2576 (1998).
  - [13] P. Papazoglou et al., Phys. Rev. **C59**, 411 (1999).
  - [14] P. Wang, V. E. Lyubovitskij, T. Gutsche, and A. Faessler, Phys. Rev. **C70**, 015202 (2004).
  - [15] V. Dexheimer, S. Schramm, and H. Stoecker, J. Phys. **G35**, 014060 (2008).
  - [16] V. Dexheimer and S. Schramm (2008), arXiv:0802.1999 [astro-ph].
  - [17] L. Bonanno, A. Drago, and A. Lavagno, Phys. Rev. Lett. **99**, 242301 (2007).
  - [18] A. Drago, M. Gibilisco, and C. Ratti, Nucl. Phys. **A742**, 165 (2004).
  - [19] J. Schechter, Phys. Rev. **D21**, 3393 (1980).

- [20] A. A. Migdal and M. A. Shifman, Phys. Lett. **B114**, 445 (1982).
- [21] E. K. Heide, S. Rudaz, and P. J. Ellis, Phys. Lett. **B293**, 259 (1992).
- [22] P. J. Ellis, E. K. Heide, and S. Rudaz, Phys. Lett. **B282**, 271 (1992).
- [23] G. E. Brown and M. Rho, Phys. Rev. Lett. **66**, 2720 (1991).
- [24] A. Mocsy, I. N. Mishustin, and P. J. Ellis, Phys. Rev. **C70**, 015204 (2004).
- [25] J. I. Kapusta and C. Gale, *Finite-temperature field theory: Principles and applications* (2006), Cambridge University Press.
- [26] M. Cheng et al., Phys. Rev. **D75**, 034506 (2007).
- [27] M. Cheng et al., Phys. Rev. **D74**, 054507 (2006).
- [28] T. C. Blum, J. E. Hetrick, and D. Toussaint, Phys. Rev. Lett. **76**, 1019 (1996).
- [29] I. C. Arsene et al., Phys. Rev. **C75**, 034902 (2007).
- [30] N. K. Glendenning and S. A. Moszkowski, Phys. Rev. Lett. **67**, 2414 (1991).
- [31] V. N. Russkikh and Y. B. Ivanov, Phys. Rev. **C74**, 034904 (2006).
- [32] H. Geissel et al., AIP Conf. Proc. **619**, 749 (2002).
- [33] E. Friedman and A. Gal, Phys. Lett. **B432**, 235 (1998).
- [34] D. Trnka et al. (CBELSA/TAPS), Phys. Rev. Lett. **94**, 192303 (2005).
- [35] R. Muto et al. (KEK-PS-E325), Phys. Rev. Lett. **98**, 042501 (2007).
- [36] V. Metag, J. Phys. **G34**, S397 (2007).
- [37] R. Nasseripour et al. (CLAS), Phys. Rev. Lett. **99**, 262302 (2007).
- [38] D. Adamova et al. (CERES/NA45), Phys. Rev. Lett. **91**, 042301 (2003).
- [39] R. Arnaldi et al. (NA60), Phys. Rev. Lett. **96**, 162302 (2006).
- [40] H. van Hees and R. Rapp (2006), hep-ph/0604269.
- [41] S. Woosley and T. Janka, Nature Physics **1**, 147 (2005).
- [42] F. D. Swesty, J. M. Lattimer, and E. S. Myra, Apj **425**, 195 (1994).
- [43] E. Baron, J. Cooperstein, and S. Kahana, Phys. Rev. Lett. **55**, 126 (1985).
- [44] A. B. Migdal, A. I. Chernoutsan, and I. N. Mishustin, Phys. Lett. **B83**, 158 (1979).
- [45] M. Takahara and S. K., Phys. Lett. **B156**, 17 (1985).
- [46] N. A. Gentile, M. B. Aufderheide, G. J. Mathews, F. D. Swesty, and G. M. Fuller, Astrophys. J. **414**, 701 (1993).
- [47] A. Drago, Nucl. Phys. **A661**, 633 (1999).
- [48] J. M. Lattimer and F. D. Swesty, Nucl. Phys. **A535**, 331 (1991).
- [49] T. Klahn et al., Phys. Rev. **C74**, 035802 (2006).
- [50] T. Janka, private communication.
- [51] T. Gaitanos et al., Nucl. Phys. **A732**, 24 (2004).
- [52] B. Liu, V. Greco, V. Baran, M. Colonna, and M. Di Toro, Phys. Rev. **C65**, 045201 (2002).
- [53] S. Typel and H. H. Wolter, Nucl. Phys. **A656**, 331 (1999).
- [54] S. Typel, Phys. Rev. **C71**, 064301 (2005).
- [55] E. N. E. van Dalen, C. Fuchs, and A. Faessler, Nucl. Phys. **A744**, 227 (2004).
- [56] E. N. E. van Dalen, C. Fuchs, and A. Faessler, Phys. Rev. Lett. **95**, 022302 (2005).
- [57] T. Gross-Boelting, C. Fuchs, and A. Faessler, Nucl. Phys. **A648**, 105 (1999).
- [58] F. de Jong and H. Lenske, Phys. Rev. **C58**, 890 (1998).
- [59] E. E. Kolomeitsev and D. N. Voskresensky, Nucl. Phys. **A759**, 373 (2005).
- [60] A. Akmal, V. R. Pandharipande, and D. G. Ravenhall, Phys. Rev. **C58**, 1804 (1998).
- [61] D. J. Nice et al., Astrophys. J. **634**, 1242 (2005).
- [62] P. Haensel, A. Y. Potekhin and D. G. Yakovlev, *Neutron stars 1: Equation of state and structure* (2007), Springer, New York.
- [63] H. Muller, Nucl. Phys. **A618**, 349 (1997).
- [64] L. McLerran and R. D. Pisarski, Nucl. Phys. **A796**, 83 (2007).
- [65] the expansion in  $\nu\Delta\nu$  is truncated at fourth order, because at low temperature  $\Delta\nu$  is small since the mass of the sigma field is large, while at large temperature the sigma field is small because chiral symmetry is (at least approximately) restored.
- [66] Following similar arguments, if  $m_\omega$  and  $m_\rho$  are generated by coupling the vector mesons to the chiral fields, as discussed in subsection IIB, the  $\sigma$  mean field increases at large  $\rho$ . Such a behavior was indeed obtained in Refs. [21, 22].